ACS Macro Letters

Letter

pubs.acs.org/macroletters

Supramolecular Polymers Formed by ABC Miktoarm Star Peptides

Yi-An Lin,[†,‡] Yu-Chuan Ou,[†] Andrew G. Cheetham,[†,‡] and Honggang Cui*[,†,‡]

[†]Department of Chemical and Biomolecular Engineering and [‡]Institute for NanoBioTechnology, The Johns Hopkins University, Baltimore, Maryland 21218, United States

Supporting Information

ABSTRACT: We report here the design and synthesis of an ABC miktoarm star peptide connecting through a lysine junction a short peptide sequence and two hydrophobic but immiscible blocks (a hydrocarbon and a fluorocarbon). The designed molecule can self-assemble into one-dimensional nanostructures with a great diversity of kinetically evolving morphologies in aqueous solution, while molecules that contain only one of the two hydrophobic blocks form structurally similar filaments. We believe the rich assembly behavior and morphological evolution are a direct reflection of the molecular frustration present within the filament core as a result of the incompatibility of the fluorocarbon and hydrocarbon segments. Our finding opens new opportunities for creating complex supramolecular polymers through the architecture design of small molecular building units.

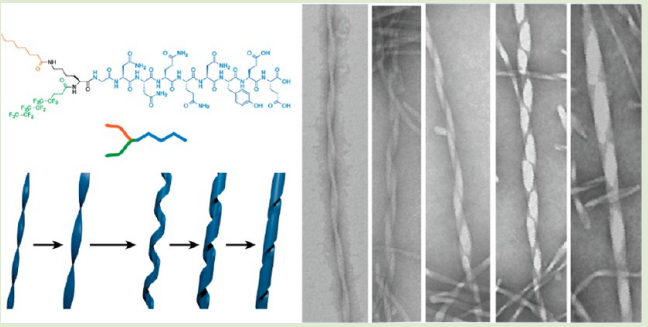

The spontaneous association of small molecules into discrete one-dimensional nanostructures with a high degree of internal order provides a facile yet effective means to construct supramolecular polymers.[1−3] Such supramolecular polymers are characterized with anisotropic growth governed by directional, noncovalent interactions, possessing interesting optical,[4,5] electrical,[6−10] or biological properties.[11−13] This bottom-up strategy has led to the creation of a plethora of functional nanomaterials, including bioactive nanofibers formed by peptide amphiphiles,[11−17] and semiconducting or photoconductive nanowires and nanotubes formed by π-conjugated molecules.[4−10] Since the macroscopic/nanoscopic properties of the resulting materials are strongly associated with the chemical structures and organization of the building blocks,[18] bridging the design rationale of building blocks and the supramolecular characteristics becomes crucial for the development of functional nanomaterials. Peptides are regarded as very effective molecular building blocks, serving as powerful bottom-up constituents to construct supramolecular polymers. Accordingly, much effort has been devoted to elucidating connections between peptide sequences and resulting supramolecular morphology.[19−21] However, design parameters for the hydrophobic segments, such as the chain architecture (branched vs linear), though being an effective strategy frequently used in polymeric systems to achieve novel morphologies,[22−25] are rarely explored for small molecular self-assembly systems. In particular, incorporation of a third immiscible component has not been exploited specifically in the design of peptidic building units. In this work, we report the first example of an ABC miktoarm star peptide that can self-assemble into a variety of complex supramolecular polymers in aqueous conditions.

For small molecules to assemble into stable, discrete, one-dimensional nanostructures that are not necessarily stabilized by a spontaneous curvature, we believe at least two criteria should be included in the molecular design. One part of the molecule should afford a strong and directional associative interaction (e.g., hydrogen bonding[14,19,26] or $\pi-\pi$ interactions[6−9,27,28]) for one-dimensional growth into stable assemblies. A second feature should also be included to limit growth in other dimensions(s) so as to form discrete assemblies. Inspired by the miktoarm star terpolymer system developed by Lodge, Hillmyer, and co-workers,[23−25] we incorporated the design principles to create supramolecular polymers formed by an ABC miktoarm star peptide, an amphiphilic molecule comprising three distinct segments linked through a lysine junction: (1) a saturated hydrocarbon, (2) a hydrophobic and lipophobic fluorocarbon, and (3) a short peptide sequence (Figure 1a). The use of two different hydrophobic blocks, immiscible with one another, could potentially offer a new mechanism to tune the morphology when the hydrophobic collapse forces these two moieties into close proximity. The peptide GNNQQNY was chosen because of its high propensity to form parallel β-sheets;[29] this seven-residue peptide is derived from the key amyloid-forming region in yeast prion Sup35, known to adopt a parallel β-sheet secondary structure in the native protein.[29] In addition, two glutamic acid residues were placed at the *C*-terminus of the peptide to impart hydrophilicity to the designed peptides.

Received: October 23, 2013
Accepted: November 26, 2013
Published: November 27, 2013

ACS Publications © 2013 American Chemical Society

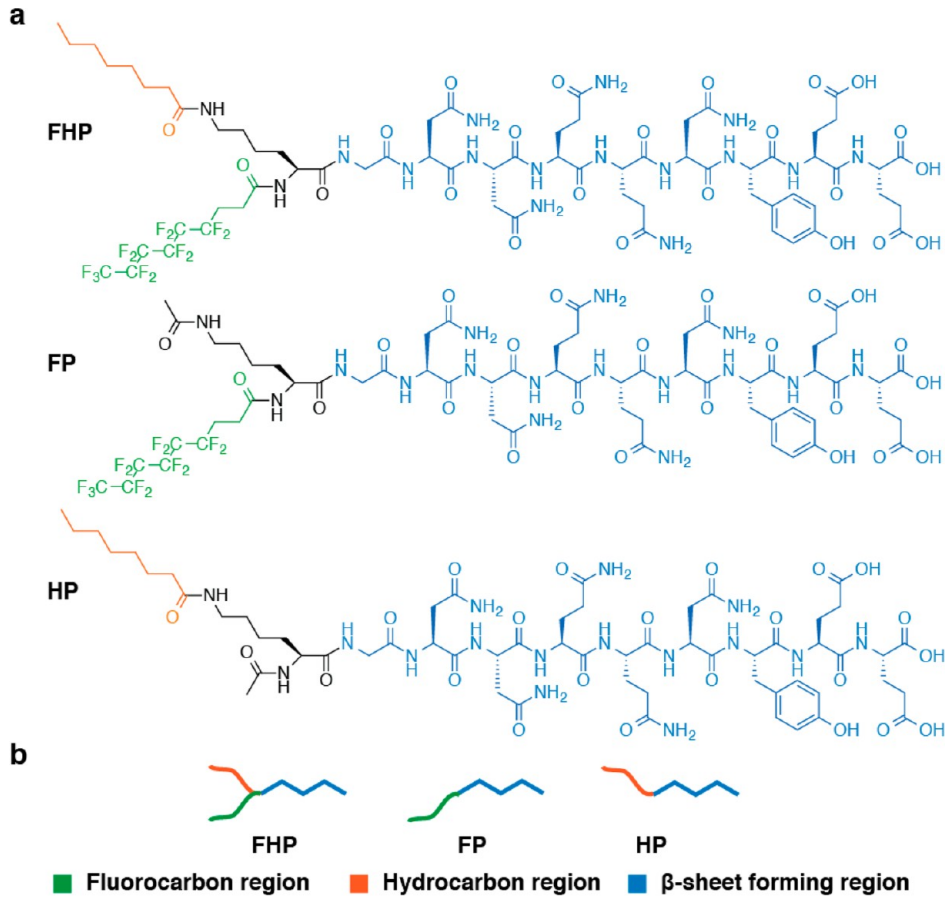

Figure 1. (a) Chemical structures and (b) schematic representations of the studied miktoarm star peptide **FHP** and the two control peptides, **FP** and **HP**, that possess only one of the two hydrophobic blocks used in this study.

The miktoarm star peptide, **FHP**, was synthesized using the standard protocols of Fmoc solid-phase peptide synthesis [see S1 in the Supporting Information (SI)]. Two control molecules (**FP** and **HP**), containing only one of the two hydrophobic moieties, were also synthesized in order to better understand the assembly behaviors of the miktoarm star peptide (Figure 1a). We first determined the critical micellization concentrations (CMC) of the three molecules using Nile red as a probe. Nile red is a lipophilic, solvatochromic dye that fluoresces intensely upon exposure to hydrophobic environments, while in aqueous media its fluorescence is strongly quenched and red-shifted.[30,31] The CMC of the studied peptides was determined by incubating these molecules at various concentrations with a fixed content of Nile red. Plotting the ratio of intensity at 635 nm (emission maximum of the encapsulated dye) to that at 660 nm (emission maximum in aqueous conditions) against the concentration of each peptide shows the transition that occurred when the peptide concentration exceeded the CMC (Figure 2a–c; complete spectra are given in Figure S4 in SI). These experiments show that **FHP**, as expected due to its greater hydrophobicity (two tails vs one), has a lower CMC value (~1 μM) than that of both **FP** and **HP** (~10 μM for both). There was no apparent difference in CMC value between **FP** and **HP**. At concentrations above their respective CMC values, all three peptide conjugates assume a β-sheet conformation in aqueous solution, as revealed by our circular dichroism (CD) spectrometric studies (Figure 2d). All three spectra are characterized by a negative peak in the 215–220 nm region

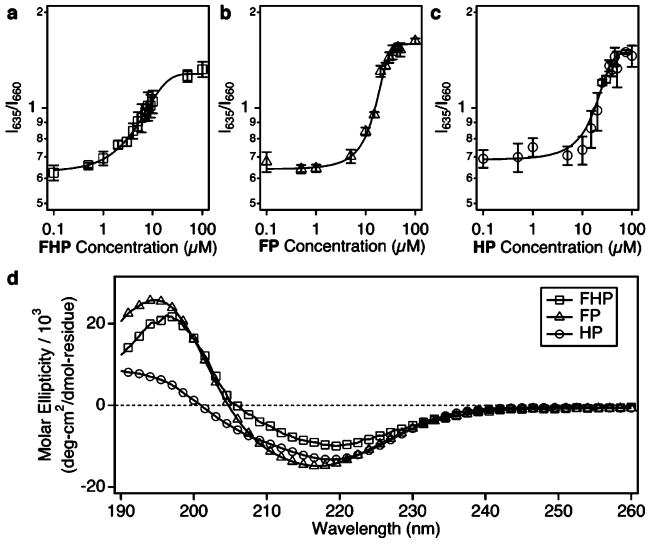

Figure 2. Determination of CMC for **FHP** (a), **FP** (b), and **HP** (c) using the Nile red encapsulation method. (d) Far-UV circular dichroism spectra of 0.1% (w/v) solutions of **FHP**, **FP**, and **HP**, respectively, all showing characteristic absorption of β-sheet assemblies.

and a positive peak around 195 nm, both signatures of the β-sheet secondary conformation.

Characterization of the assembled nanostructures in aqueous solutions was accomplished using both transmission electron

dx.doi.org/10.1021/mz400535g | ACS Macro Lett. 2013, 2, 1088–1094

microscopy (TEM) and cryogenic-TEM (cryo-TEM). Regular TEM imaging of negatively stained samples offers a relatively higher resolution, while cryo-TEM enables direct imaging of nanostructures embedded in a thin layer of vitrified sample. Figure 3 depicts TEM and cryo-TEM micrographs of

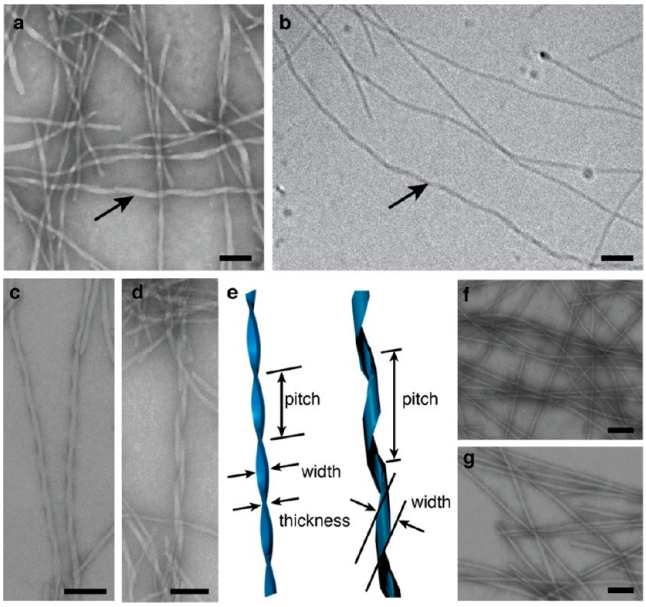

Figure 3. Representative TEM and cryo-TEM micrographs of the designed peptides. TEM (a) and cryo-TEM (b) micrographs collected from a 0.1% **FHP** aqueous solution after one day aging. The narrow helical ribbons were indicated by arrows in both panels. Representative TEM images of twisted ribbons (c) and helical ribbons (d) observed in 0.1% **FHP** aqueous solution after one day of aging. Schematic representations of two major types of one-dimensional structure, a twisted ribbon (left) and a helical ribbon (right) (e). Representative TEM micrographs of the filaments formed by **FP** (f) and **HP** (g) at 0.1% aqueous solutions aged for 1 day. All bars = 100 nm.

nanostructures formed by **FHP**, **FP**, and **HP** after one day of incubation. The one-dimensionality of the observed nanostructures was interpreted to result from the intermolecular hydrogen bonding among the peptide units, in accordance with our CD measurements.

Two major types of filaments were identified for **FHP** assemblies in both TEM and cryo-TEM imaging, twisted ribbons and helical ribbons, after one day of aging, with twisted ribbons observed much more frequently (Figure 3a–d). Supramolecular structures of **FHP** identified as twisted ribbons were those comprising a periodic pitch and twisting with a rotation direction perpendicular to the long axis of the ribbon (Figure 3c). We noted that the thickness of these twisted ribbons (measured from regular TEM micrographs) was on average ∼15 nm, a value that is larger than the expected thickness of a partially or fully interdigitated bilayer, implying the observed ribbons may consist of multiple stacked layers. The pitch of the twisted ribbons measured from TEM micrographs was ∼90 nm. Helical ribbons of **FHP** could be distinguished from the twisted ribbons as their distinct two-dimensional projections were clearly visible in both TEM and cryo-TEM imaging (Figure 3a,b,d). The observed narrow helical ribbons have a pitch on the order of hundreds of nanometers and a ribbon width of ∼30 nm.

Both **FP** and **HP** were also found to form filamentous structures in aqueous solutions. For **FP**, both twisted ribbons (twisting with periodic pitch) and single filaments (no obvious pitch) were observed to be the dominant nanostructures. The twisted ribbons formed by **FP** possess thicknesses that are almost identical to the size of the single filaments (7.0 ± 1.4 nm), suggesting the ribbons could be the intertwined form of the single filaments. **HP** assembled into fibers with a width of 13.6 ± 2.5 nm, a dimension close to the doubled value of the estimated length of the fully extended peptides (assuming a β-sheet conformation), inferring that **HP** assembles in a core–shell manner. This molecular arrangement is in consistency with the proposed core–shell cylindrical structure formed by the majority of reported peptide amphiphiles.[12,32,33]

For self-assembling systems in which building blocks possess strong intermolecular interactions, the observed morphologies are often only kinetically stable at the experimental time scale and could potentially evolve into thermodynamically more stable structures at later stages. Short- or long-term aging, for instance, can lead to the transformation of twisted ribbons into helical coils or nanotubes.[34−37] We therefore investigated the kinetic evolution of the assemblies formed by the miktoarm star peptide **FHP**, and observed significant changes in the supramolecular structures after aging the solution for 6 months. First of all, a general increase in width was evident for twisted ribbons from both TEM and cryo-TEM imaging upon aging (Figure 4a,b and Figure S5 in SI). Second, the pitch and thickness of the twisted ribbons were also found to increase over time (Figures 4c,d). The thickness of the ribbons formed by **FHP** could be up to ∼30 nm (averaged thickness ∼20 nm), implying that time-dependent molecular stacking also took place in this dimension. We also found that there is an approximate linear correlation between thickness and pitch and between width and pitch for these twisted ribbons, suggesting that the evolution of twisted ribbons observed here may be similar to the process of hierarchical assemblies formed by chiral rod-like molecules rich in β-strands.[38] Third, helical ribbons were much more frequently observed after aging, accompanied with an increase in dimensions (Figures 4e,f and 5).

Closer examination further reveals that the helical ribbons generally possess widths above 30 nm, while the twisted ribbons usually comprise widths less than this value (Figure 4c). In addition, several TEM images seem to capture a number of intermediate structures that were in the process of converting from twisted ribbons to helical ribbons (Figure 4g, and S5b), and these intermediate structures seldom possess a width greater than 30 nm. These observations indicate that there might exist a critical value in ribbon width above which twisted ribbons would commence to transform into helical ribbons. The twisted ribbon-to-helical transformation has been reported possible through theoretical simulation,[39] and also in experimental work where the morphological transition was ascribed to the chiral instability of twisted ribbons during the widening process.[34−37] These results led us to propose the possible mechanism shown in Figure 5b, the illustration depicting the transformation from twisted ribbons to helical ribbons. Despite precedent studies indicating the possibility for helical ribbons to transform into tubules during the width-widening process,[35,40] there were no indication for forming tubular structures in our system.

Interestingly, a third type of large one-dimensional structures was also frequently spotted for **FHP** samples aged for 6

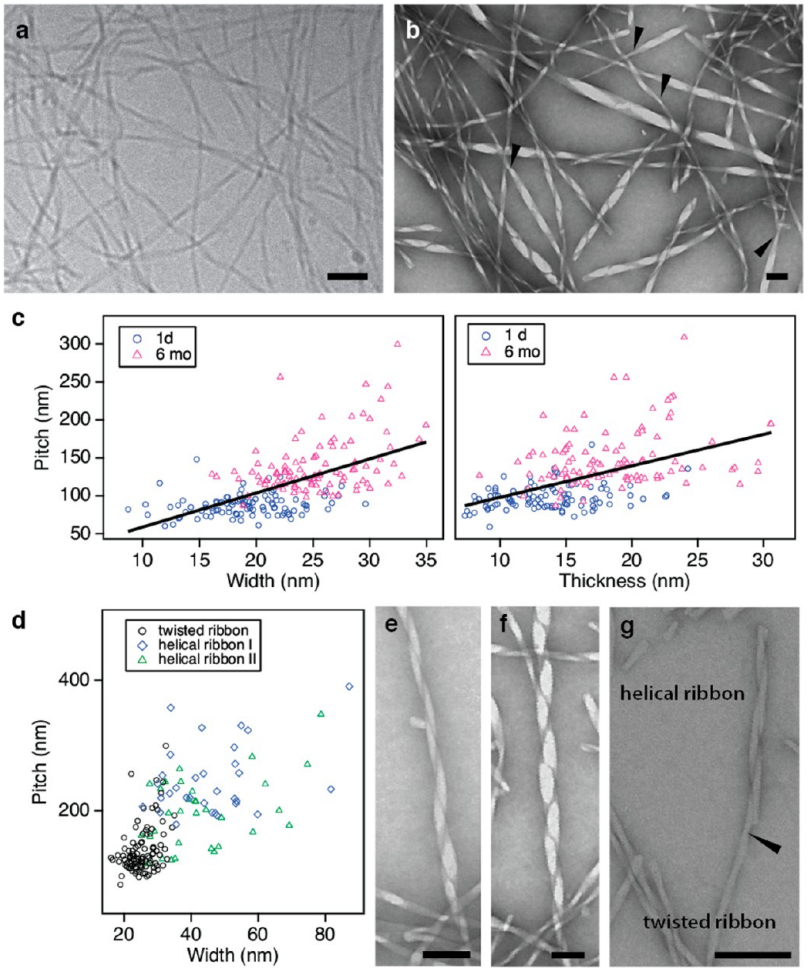

Figure 4. Kinetic evolution of the supramolecular polymers formed by **FHP** after aging the samples for 6 months. Representative cryo-TEM (a) and TEM (b) micrographs collected from a 0.1% **FHP** aqueous solution aged for 6 months. Arrows in panel b indicate the twisted-to-helical transitions of intermediate structures. (c) Scatter charts of the correlation between ribbon pitch and width (left), and the correlation between ribbon pitch and thickness (right) measured for twisted ribbons from a 0.1% **FHP** aqueous solution that was aged for 1 day or 6 months. (d) Correlation between the pitch and width for twisted ribbons, type I helical ribbons and type II helical ribbons formed by **FHP** after 6 month aging. n = 100 for twisted ribbons and n = 30 for type I and type II helical ribbons. Representative TEM images of helical ribbons (e, f) and an intermediate twisted-to-helical ribbon (g) after a 6 month aging, where the black arrow indicates the transition point. All bars = 100 nm.

months, referred here as "type II helical ribbons", with alternating contrast along the long axis (Figure 5c−e, topological analysis in Figure 5f and Figure S6). The type II helical ribbons generally possess a width greater than 30 nm and in several cases up to ∼100 nm (Figure 5a). The fraction of helical ribbon II out of the total nanostructures observed was approximately 51.8% on the basis of our statistics from 10 TEM images (total count: 251). It is important to note that all the samples prepared for regular TEM imaging in this study were stained with a 3% (w/v) uranyl acetate aqueous solution and, as a consequence, the contrast mechanism of the collected TEM micrographs is primarily dominated by the staining reagent, with the brightest areas generally having the least deposition of the uranyl ions. Unlike helical ribbons discussed previously (type I) that demonstrate bright spots symmetrically located on both sides (Figure 4e,f), the type II helical ribbons reveal only alternating bright spots and gray regions along the ribbon's long axis (Figure 5c−e).

However, there are several common features between type II and type I helical ribbons: first, the type II helical ribbons possess a similar width-and-pitch relation to that of type I helical ribbons (Figure 4c). Second, intermediate structures were also spotted revealing morphological transition from twisted ribbons to type II helical ribbons within the same filamentous nanostructures (Figure 5g). In addition, both type I and type II helical ribbons exhibit the right-handed supramolecular chirality, evidenced by both TEM and AFM imaging (Figure S6). It should be noted that the supramolecular chirality could only be determined from TEM micrographs if the orientations of the grids of the negatively stained specimens were known with respect to the electron beam traveling direction. These observations suggest that type II and type I helical ribbons are likely the same structures in origin. The distinct contrast between the two structures observed in TEM images (collected from samples stained with uranyl ions) could originate from the difference in the deposition of the staining agents. We speculate that type II helical ribbons are likely the later stage assemblies of the type I helical ribbons with both increased thickness and widths. Their more robust structures due to the increased thickness would prevent the collapse of the ribbon structure during the sample preparation while the increased width likely prevents the deposition of the uranyl ions into the tubular inner channels, leading to formation of different contrast patterns in TEM images. Occasionally, we

dx.doi.org/10.1021/mz400535g | *ACS Macro Lett.* 2013, 2, 1088−1094

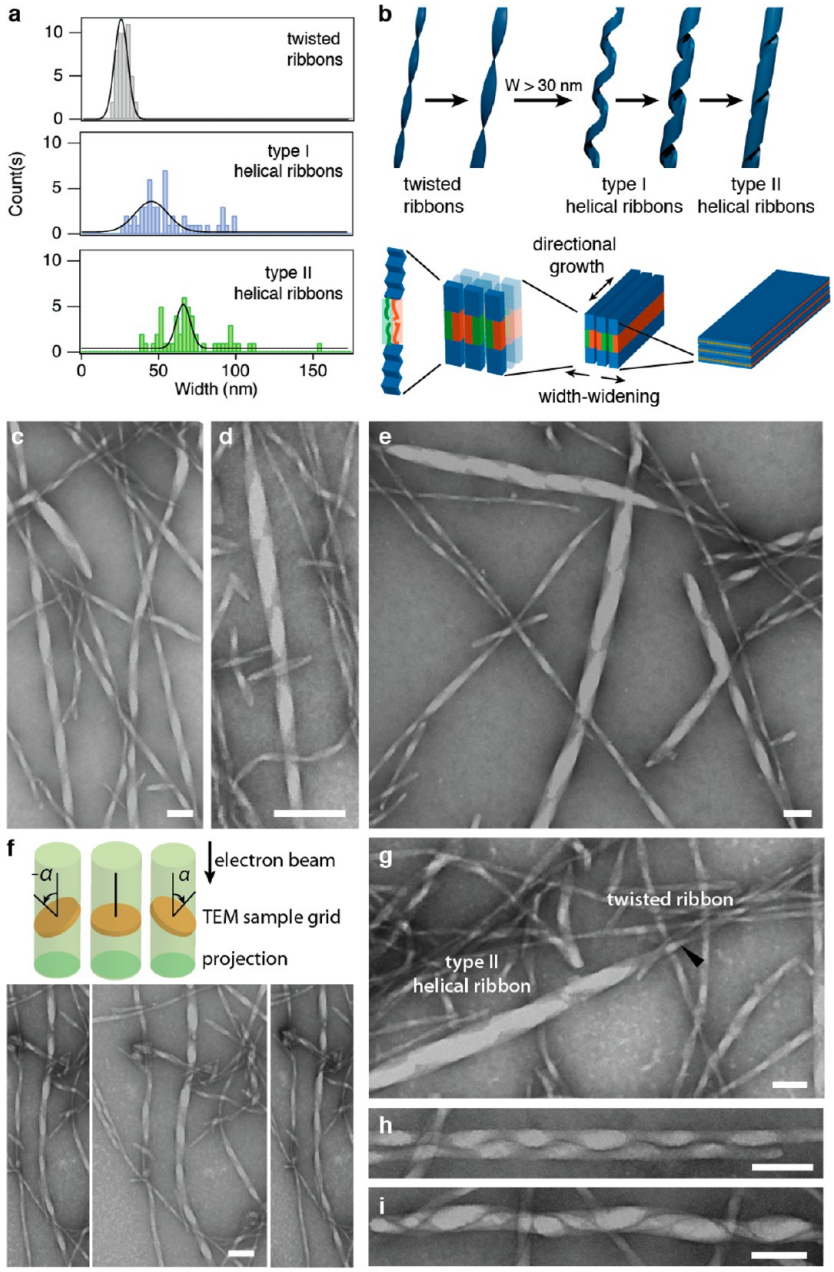

Figure 5. (a) Statistical width distribution of twisted ribbons, helical ribbons I and helical ribbons II after aging the solution for 6 months (n = 50 for each ribbon type). A Gaussian distribution fits the data (black curves). (b) The proposed transition mechanisms from twisted ribbons to helical ribbons and the possible pathways for the observed pitch and width variations associated with sample aging (top), and also a proposed model for the chain packing within the observed FHP helical ribbons (bottom). (c–e) Representative TEM micrographs of the type II helical ribbons formed by **FHP** after aging 6 months, displaying the right-handedness according to the uranyl accumulation on the surface. (f) Topological analysis in TEM for a type II helical ribbon formed by **FHP**. Top panel depicts the instrumentation setup for the topological studies. Bottom panels display the projection of a type II helical ribbon while the specimen is tilted in TEM column. Tilt angle α is −45°, 0°, and 45° for the left, middle, and right panels. (g–i) TEM micrographs of an intermediate structure bearing twisted ribbon and type II helical ribbon (panel g, the arrow indicates the transition), and intertwining one-dimensional structures (h, i). All bars = 100 nm.

could observe two or more of these structures interact or intertwine with each other to form more complex, higher hierarchical assemblies (Figures 5h,i).

In contrast to the rich assembly behaviors of the **FHP** peptide, the two control molecules, **FP** and **HP**, did not exhibit any obvious morphological changes after 6 months of aging (Figure S7 in SI). Replacing the fluorocarbon segment of **FHP** with a hydrocarbon gave an amphiphile ($\mathbf{H_2P}$) that was observed to assemble into nanofibers similar to those formed by **HP**, and that did not show any kinetically dependent assembly behavior (see Figure S9 in SI).

These results clearly suggest that the difference in self-assembly among **FHP**, **FP**, and **HP**, and, in particular, the observation of a variety of different supramolecular polymers formed by **FHP**, is directly linked to the immiscibility between the hydrocarbon and fluorocarbon segments within the **FHP** assemblies. Though this immiscibility has been reported to lead the ABC miktoarm star terpolymers to form chemically distinct multicompartments within polymeric micelles,[23,24] there was

dx.doi.org/10.1021/mz400535g | *ACS Macro Lett.* 2013, 2, 1088–1094

no direct observation of multiple compartments within the formed one-dimensional nanostructures in our case. Given the extremely short lengths of the used fluorocarbon and hydrocarbon, it might be impossible to access the separate domains comprising only hydrocarbons or fluorocarbons (Figure 5b). However, we did observe, particularly in the sample aged for six months, that the width of the **FHP** assemblies could vary dramatically within a single filament (Figures 4 and 5). Amyloid peptides are well-known to form polymorphic filaments of varying twists and widths; however, their width is often consistent across a large length scale within a particular filament. The heavily fluctuating width observed within a single filament in our system manifest again the effect of having two immiscible hydrophobic chains in the molecular design.

Although the studied system is concerned with small molecular building units, it bears some resemblance to a polymeric system. It has been shown by several laboratories that small molecules could demonstrate kinetically controlled aggregation behaviors similar to the macromolecular assemblies.[34−36,41−43] Our system appears to be another example where kinetic evolution plays a critical role in the creation of supramolecular polymers. More importantly, our results suggest a subtle change in the molecular design could lead to a profound effect on the assembled nanostructures. In polymeric assembly systems, the segregation force between different polymer chains is determined by the dimensionless product χN, where χ is the Flory−Huggins interaction parameter describing the interactions between two different monomers and N is the degree of polymerization. In our oligomer system, while χ could be relatively large due to the strong incompatibility between fluorocarbons and hydrocarbons,[44] N is an extremely small number (only involving six fluorocarbons in our system, N = 3). Therefore, the product χN would be too small to lead to any significant chain segregation and, thus, may not be used to explain exclusively the observed morphological difference. However, the observation that this subtle immiscibility can induce a dramatic change in the assembly landscape to produce a wide variety of interesting nanostructures is, therefore, truly remarkable and points to the vast potential of the molecular design in low-molecular-weight building units for the development of supramolecular materials.

In summary, we have presented a design of branched peptide that possesses both fluorocarbon and hydrocarbon segments. These immiscible chains lead to the spontaneous formation of complex supramolecular polymers that exhibit a time-dependent evolution from twisted ribbons to helical ribbons. The design of architecture for small molecular building units could provide an effective approach to construct alternative morphologies with similar surface chemistry through the incorporation of different hydrophobic or lipophobic segments.

■ ASSOCIATED CONTENT

Ⓢ Supporting Information

Synthesis of all peptides, experimental procedure, and detailed characterizations. This material is available free of charge via the Internet at http://pubs.acs.org.

■ AUTHOR INFORMATION

Corresponding Author

*E-mail: hcui6@jhu.edu.

Notes

The authors declare no competing financial interest.

■ ACKNOWLEDGMENTS

The authors thank Dr. Kalina Hristova for the use of the spectropolarimeter and fluorimeter instrumentation, Dr. Ankur Verma and Dr. Rebecca Schulman for the assistance with AFM imaging, and Dr. J. Michael McCaffery for assistance with TEM and cryo-TEM imaging. We gratefully acknowledge financial support from the JHU Startup Grant, National Institutes of Health (NIH), for funding Y.-A.L. (R25CA153952) and A.G.C. (T-32CA130840), and National Science Foundation (CHE-0840463) for the purchase of the MALDI-ToF mass spectrometer used in this work.

■ REFERENCES

(1) Aida, T.; Meijer, E. W.; Stupp, S. I. *Science* **2012**, *335* (6070), 813−817.
(2) De Greef, T. F. A.; Smulders, M. M. J.; Wolffs, M.; Schenning, A.; Sijbesma, R. P.; Meijer, E. W. *Chem. Rev.* **2009**, *109* (11), 5687−5754.
(3) Brunsveld, L.; Folmer, B. J. B.; Meijer, E. W.; Sijbesma, R. P. *Chem. Rev.* **2001**, *101* (12), 4071−4097.
(4) Zang, L.; Che, Y. K.; Moore, J. S. *Acc. Chem. Res.* **2008**, *41* (12), 1596−1608.
(5) Kim, F. S.; Ren, G. Q.; Jenekhe, S. A. *Chem. Mater.* **2011**, *23* (3), 682−732.
(6) Yamamoto, Y.; Fukushima, T.; Suna, Y.; Ishii, N.; Saeki, A.; Seki, S.; Tagawa, S.; Taniguchi, M.; Kawai, T.; Aida, T. *Science* **2006**, *314* (5806), 1761−1764.
(7) Wall, B. D.; Diegelmann, S. R.; Zhang, S. M.; Dawidczyk, T. J.; Wilson, W. L.; Katz, H. E.; Mao, H. Q.; Tovar, J. D. *Adv. Mater.* **2011**, *23* (43), 5009−5014.
(8) Ajayaghosh, A.; George, S. J. *J. Am. Chem. Soc.* **2001**, *123* (21), 5148−5149.
(9) Ma, M.; Kuang, Y.; Gao, Y.; Zhang, Y.; Gao, P.; Xu, B. *J. Am. Chem. Soc.* **2010**, *132* (8), 2719−2728.
(10) Hoeben, F. J. M.; Jonkheijm, P.; Meijer, E. W.; Schenning, A. *Chem. Rev.* **2005**, *105* (4), 1491−1546.
(11) Silva, G. A.; Czeisler, C.; Niece, K. L.; Beniash, E.; Harrington, D. A.; Kessler, J. A.; Stupp, S. I. *Science* **2004**, *303* (5662), 1352−1355.
(12) Black, M.; Trent, A.; Kostenko, Y.; Lee, J. S.; Olive, C.; Tirrell, M. *Adv. Mater.* **2012**, *24* (28), 3845−3849.
(13) Stupp, S. I. *Nano Lett.* **2010**, *10* (12), 4783−4786.
(14) Hamley, I. W. *Soft Matter* **2011**, *7* (9), 4122−4138.
(15) Branco, M. C.; Sigano, D. M.; Schneider, J. P. *Curr. Opin. Chem. Biol.* **2011**, *15* (3), 427−434.
(16) Matson, J. B.; Stupp, S. I. *Chem. Commun.* **2012**, *48* (1), 26−33.
(17) Yu, Y. C.; Berndt, P.; Tirrell, M.; Fields, G. B. *J. Am. Chem. Soc.* **1996**, *118* (50), 12515−12520.
(18) Whitesides, G. M.; Grzybowski, B. *Science* **2002**, *295* (5564), 2418−2421.
(19) Paramonov, S. E.; Jun, H. W.; Hartgerink, J. D. *J. Am. Chem. Soc.* **2006**, *128* (22), 7291−7298.
(20) Geisler, I. M.; Schneider, J. P. *Adv. Funct. Mater.* **2012**, *22* (3), 529−537.
(21) Hong, Y. S.; Legge, R. L.; Zhang, S.; Chen, P. *Biomacromolecules* **2003**, *4* (5), 1433−1442.
(22) Bates, F. S.; Hillmyer, M. A.; Lodge, T. P.; Bates, C. M.; Delaney, K. T.; Fredrickson, G. H. *Science* **2012**, *336* (6080), 434−440.
(23) Li, Z. B.; Kesselman, E.; Talmon, Y.; Hillmyer, M. A.; Lodge, T. P. *Science* **2004**, *306* (5693), 98−101.
(24) Li, Z. B.; Hillmyer, M. A.; Lodge, T. P. *Nano Lett.* **2006**, *6* (6), 1245−1249.
(25) Li, Z.; Hillmyer, M. A.; Lodge, T. P. *Langmuir* **2006**, *22* (22), 9409−9417.

(26) Smeenk, J. M.; Otten, M. B. J.; Thies, J.; Tirrell, D. A.; Stunnenberg, H. G.; van Hest, J. C. M. *Angew. Chem., Int. Ed.* **2005**, *44* (13), 1968−1971.
(27) Burattini, S.; Greenland, B. W.; Merino, D. H.; Weng, W.; Seppala, J.; Colquhoun, H. M.; Hayes, W.; Mackay, M. E.; Hamley, I. W.; Rowan, S. J. *J. Am. Chem. Soc.* **2010**, *132* (34), 12051−12058.
(28) Yang, W. Y.; Lee, E.; Lee, M. *J. Am. Chem. Soc.* **2006**, *128* (11), 3484−3485.
(29) Nelson, R.; Sawaya, M. R.; Balbirnie, M.; Madsen, A. O.; Riekel, C.; Grothe, R.; Eisenberg, D. *Nature* **2005**, *435* (7043), 773−778.
(30) Rexeisen, E. L.; Fan, W.; Pangburn, T. O.; Taribagil, R. R.; Bates, F. S.; Lodge, T. P.; Tsapatsis, M.; Kokkoli, E. *Langmuir* **2010**, *26* (3), 1953−1959.
(31) Greenspan, P.; Mayer, E. P.; Fowler, S. D. *J. Cell Biol.* **1985**, *100* (3), 965−973.
(32) Palmer, L. C.; Stupp, S. I. *Acc. Chem. Res.* **2008**, *41* (12), 1674−1684.
(33) Hartgerink, J. D.; Beniash, E.; Stupp, S. I. *Science* **2001**, *294* (5547), 1684−1688.
(34) Pashuck, E. T.; Stupp, S. I. *J. Am. Chem. Soc.* **2010**, *132* (26), 8819−8821.
(35) Ziserman, L.; Lee, H. Y.; Raghavan, S. R.; Mor, A.; Danino, D. *J. Am. Chem. Soc.* **2011**, *133* (8), 2511−2517.
(36) Ziserman, L.; Mor, A.; Harries, D.; Danino, D. *Phys. Rev. Lett.* **2011**, *106* (23), 4.
(37) Adamcik, J.; Castelletto, V.; Bolisetty, S.; Hamley, I. W.; Mezzenga, R. *Angew. Chem., Int. Ed.* **2011**, *50* (24), 5495−5498.
(38) Aggeli, A.; Nyrkova, I. A.; Bell, M.; Harding, R.; Carrick, L.; McLeish, T. C. B.; Semenov, A. N.; Boden, N. *Proc. Natl. Acad. Sci. U.S.A.* **2001**, *98* (21), 11857−11862.
(39) Selinger, R. L. B.; Selinger, J. V.; Malanoski, A. P.; Schnur, J. M. *Phys. Rev. Lett.* **2004**, *93* (15), 158103.
(40) Schnur, J. M.; Ratna, B. R.; Selinger, J. V.; Singh, A.; Jyothi, G.; Easwaran, K. R. K. *Science* **1994**, *264* (5161), 945−947.
(41) Korevaar, P. A.; George, S. J.; Markvoort, A. J.; Smulders, M. M. J.; Hilbers, P. A. J.; Schenning, A.; De Greef, T. F. A.; Meijer, E. W. *Nature* **2012**, *481* (7382), 492−496.
(42) Lohr, A.; Wurthner, F. *Angew. Chem., Int. Ed.* **2008**, *47* (7), 1232−1236.
(43) Wolffs, M.; Korevaar, P. A.; Jonkheijm, P.; Henze, O.; Feast, W. J.; Schenning, A.; Meijer, E. W. *Chem. Commun.* **2008**, *38*, 4613−4615.
(44) Hillmyer, M. A.; Lodge, T. P. *J. Polym. Sci., Part A: Polym. Chem.* **2002**, *40* (1), 1−8.